5

Land-Surface Classification with Unevenness and Reflectance Taken into Consideration

In this chapter, we describe an adaptive system to classify land surface by taking unevenness and reflectance into consideration. We deal with interferograms on the basis of the complex-valued Markov random field (CMRF) model in statistics. We generate an adaptively segmented map in terms of the complex-valued texture of land-surface reflection by using the complex-valued self-organizing map (CSOM) that processes CMRF-based feature vectors.

5.1 Interferometric Radar

Figure 5.1 illustrates airborne or satellite radar observation to detect reflection from the earth's surface. By employing phase-sensitive electronics, we can obtain not only the amplitude but also the phase of the reflected electromagnetic wave. As a result, we acquire an image having complex-valued pixel values. These types of radars are called interferometric radars. We can detect the phase value of a signal by mixing the signal wave with a reference wave to observe their interference. For simplicity, in Fig.5.1, we show a system in which we transmit one of the waves, capture the reflection, and mix it with the other wave to obtain the phase[1].

Roughly speaking, the amplitude represents the reflectance since it gives the power of the reflected wave. On the other hand, the phase represents the distance. That is, when the reflecting object approaches, the phase is advanced since the number of waves existing in the propagation path between the antenna and the object is reduced. Contrarily, when the object recedes,

[1] In actual airborne or satellite interferometric radars, we prepare two antennas or navigation routes, and we look aside to obtain the phase difference of the two electromagnetic waves having slightly different off-nadia angles (angle between vertical line and the radio beam). Therefore, the wavelength of the transmitted wave does not correspond to 2π in the phase value in the phase image. However, we consider the system shown in Fig.5.1 for simplicity.

A. Hirose: Complex-Valued Neural Networks, SCI 400, pp. 103–111.
springerlink.com

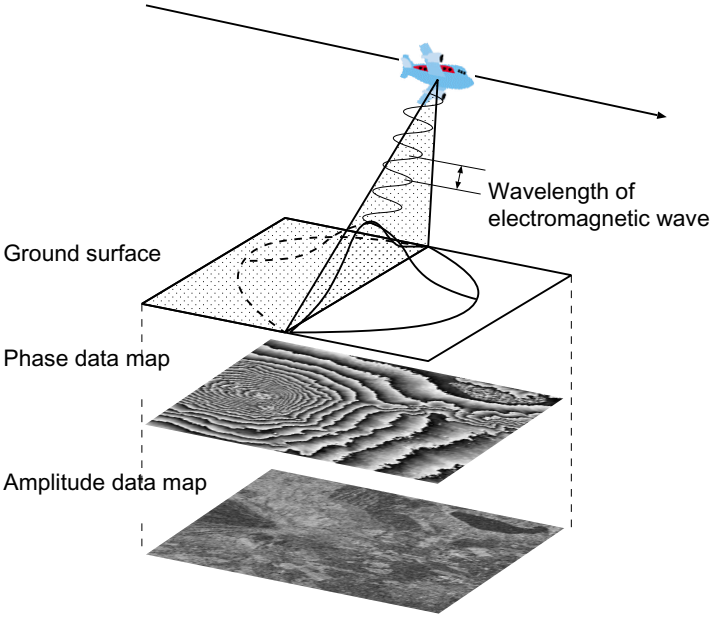

Fig. 5.1 Acquisition of land-surface information with an interferometric radar system.

the phase is retarded. Therefore, the phase represents the distance to the object, though the phase is expressed as modulo 2π. Then the phase fluctuation corresponds to surface unevenness. Slopes and fine fluctuation also change the reflection amplitude because it changes the reflection direction, or causes scattering.

In this chapter, we present a neural system that generates highly useful land-surface classification maps[197],[198]. It evaluates the texture in complex-valued reflection images that conveys reflectance and unevenness information. With this system, we can extract not only forests, deserts, lakes, and other regions having specific reflectance, but also mountain areas, ridges, spurs, rock fields, and so on, reflecting characteristic unevenness. The system is based on the complex-valued self-organizing map (CSOM) described in Section 4.5.

5.2 CMRF Model

Figure 5.2 shows an example of images obtained by an interferometric synthetic-aperture radar (InSAR) observing at around Mount Fuji. Figure 5.2(a) shows the amplitude, while Fig.5.2(b) gives the phase in modulo 2π, both in gray scale. (These original data were provided by courtesy of Dr. Masanobu Shimada of NASDA, which is presently JAXA.)

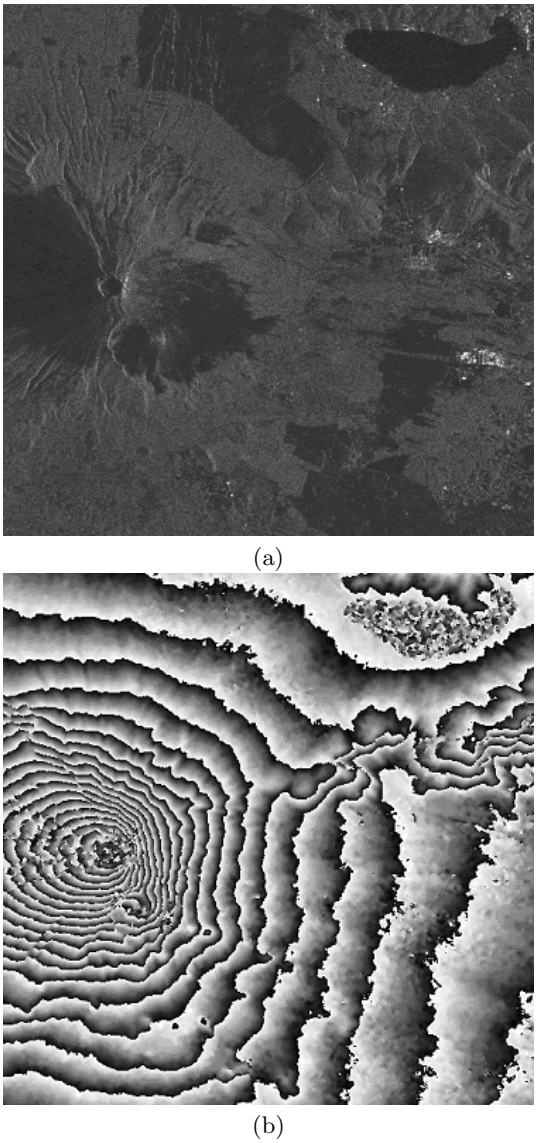

(a)

(b)

Fig. 5.2 (a)Amplitude and (b)phase of land-surface reflection obtained by an InSAR system. Reprinted from Fig.3 in [197]: Andriyan Bayu Suksmono and Akira Hirose, Adaptive complex-amplitude texture classifier that deals with both height and reflectance for interferometric SAR images, IEICE Trans. on Electron., E83-C (12):1912–1916, 2000, with permission from IEICE.

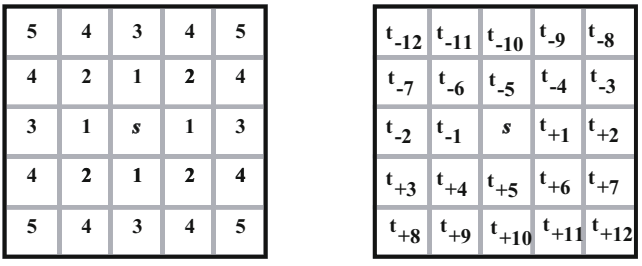

(a) (b)

Fig. 5.3 Pixel at position s to which we pay attention and its neighbors in the vicinity N_s where the neurons are (a)labeled by distance from s and (b)labeled sequentially as t_i.

Conventional adaptive segmentation systems have utilized the texture in amplitude only. In this chapter, we use the phase information as well to generate more useful segmentation maps.

We evaluate local complex-valued texture quantitatively, but as simply as possible, to classify local areas and segment the image. We consider the complex-valued Markov random field (CMRF) model. In the present process, we introduce a noncausal CMRF model, i.e., unlike the time-sequential one, having no cause and result directions. Such a model is usually suitable for images.

We deal with complex-valued images based on the noncausal CMRF model as follows. Figure 5.3 shows the assignment of pixels. The value of the pixel at position s is $z_s \in \boldsymbol{C}$. Since an observed actual image is a part of nature, we consider that it has the Markovianity. That is to say, the pixel value z_s has some relationship statistically with the values of neighbors. The nearest pixels labeled as "1" must have a strong relationship, while far pixels labeled as "4" or "5" will have a weaker one. Moreover, when the statistical characteristic is uniform in a certain area, we can expect almost identical relationship statistically even if we pay attention to another pixel in the area.

Figure 5.3(b) shows a vicinity of the pixel at position s, N_s, with local neighbors labeled as t_i. Let us consider the probability distribution $P(z_s)$ that the pixel s has a value z_s in statistics. Then we have

$$P(z_s|\text{ values of pixels in the image except for } s\ ) = P(z_s|z_{t_i} \in N_s) \quad (5.1)$$

In other words, the probability distribution is determined by the neighbors, and is unchanged within the area having a uniform statistics. The probability distribution represents a set of features of the area in the image. This is the basic idea of the CMRF.

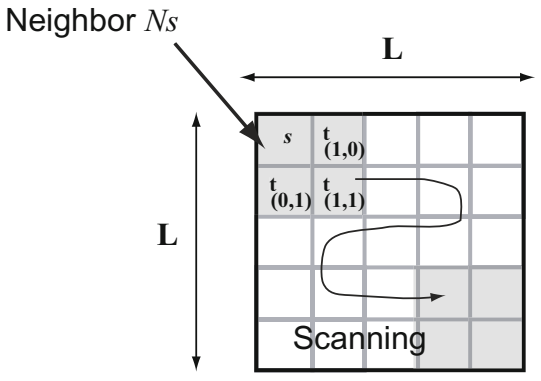

Fig. 5.4 Neighbors of point s, $t_{+1} \equiv t_{(1,0)}$, $t_{+5} \equiv t_{(0,1)}$, and $t_{+6} \equiv t_{(1,1)}$, sweep a local area having a size of $L \times L$ to gather the statistical features.

5.3 CMRF Model and Complex-Valued Hebbian learning Rule

Incidentally, (5.1) can be interpreted as follows. For statistically uniform data, the correlation between a pixel value z_s and a neighbor's values z_t is unchanged. Therefore, as mentioned in Section 4.6 (MRF estimation), we can obtain correlations between pixels by assigning a neuron to each pixel, and by making the neural connections learn the correlations with the complex-valued Hebbian rule as $< z_s(z_t)^* >$.

We assign neurons to the pixels one to one. The neurons are connected with the neighbors, and each neural connection learns the correlation between the input signals as $< z_s(z_t)^* >$. As shown in Fig.5.3, let us consider a small neighbor consisting of three pixels, $t_{+1} \equiv t_{(1,0)}$, $t_{+5} \equiv t_{(0,1)}$, and $t_{+6} \equiv t_{(1,1)}$. When the neurons *see* various, but statistically identical, images, the correlations, $< z_s(z_{t_{(1,0)}})^* >$, $< z_s(z_{t_{(0,1)}})^* >$, and $< z_s(z_{t_{(1,1)}})^* >$, will converge at certain values, respectively.

Alternatively, we can replace the temporal accumulation by a spatial one. Let us consider a local area having a size of $L \times L$ in which the statistics is uniform. Neurons in the area communicate to one another to accumulate statistical characteristics spatially. We may have a picture that the point s and the neighbors $t_{(0,1)}$, $t_{(1,0)}$, and $t_{(1,1)}$ sweep the local area with their relative location fixed. Then the neural connections memorize the following correlations

$$K(\xi, \eta) = \frac{1}{L^2} \sum_{i'=0}^{L-1} \sum_{j'=0}^{L-1} (z(i', j'))^* \ z(i' - \xi, j' - \eta) \tag{5.2}$$

where $(\xi, \eta) = \{(1,0), (0,1), (1,1)\}$.

We construct the network to gather the statistical features in the local area as described above. Other neurons, that see another area having another statistics, will memorize the correlations specific to that area. Then we can segment the image based on the correlation values accumulated in the neural connections. In the present case, the pixel values are represented by complex numbers. Therefore, the correlations reflect both the changes in reflectance (included mainly in amplitude) and the unevenness (in phase), i.e., complex texture in total. We conduct the segmentation based on the complex texture.

5.4 Construction of CSOM Image Classification System

We classify local areas into classes based on statistics adaptively by using the complex-valued self-organizing map (CSOM) mentioned in Section 4.5. Resultantly, we segment the land-surface by taking the reflectance and unevenness into consideration. In general, a SOM is widely used in adaptive vector quantization. In the present system, we expect that the CSOM also quantizes the texture-based features and segments the image into classes adaptively.

Figure 5.5 shows the construction of the CSOM-based radar system to segment a complex-valued image into classes adaptively by paying attention to the complex texture [197]. The expected function is the segmentation of landscape into, for example, Mount Fuji and Lake Yamanaka as if we had phase-sensitive eyes as mentioned in Chapter 1.

We place a local window block having a size of $L \times L$, and scan the image with this block. First, we unwrap the phase values $z(i, j)$ in the block (see Chapter 7) in a simple way. Then we obtain statistical properties such as mean M and covariance $K(\xi, \eta)$ to construct a feature vector $\boldsymbol{K}$ to be fed to the CSOM as

$$\boldsymbol{K} \equiv [M, K(0,0), K(0,1), K(1,0), K(1,1)] \tag{5.3}$$

$$M = \frac{1}{L^2} \sum_{i=0}^{L-1} \sum_{j=0}^{L-1} z(i,j) \tag{5.4}$$

$$K(\xi, \eta) = \frac{1}{L^2} \sum_{i=0}^{L-1} \sum_{j=0}^{L-1} (z(i,j))^* \ z(i+\xi, j+\eta) \tag{5.5}$$

where $(\cdot)^*$ means complex conjugate. Consequently, the covariance $K(\xi, \eta)$ includes phase differences, reflecting the height variation, unevenness, and their texture. Therefore, the system can estimate whether an amplitude change is caused by a change in reflectance, or by a change in unevenness.

Moreover, we can introduce some concepts such as "mountain" and "valley" as new indices for classification. In this case, the directions of slopes are

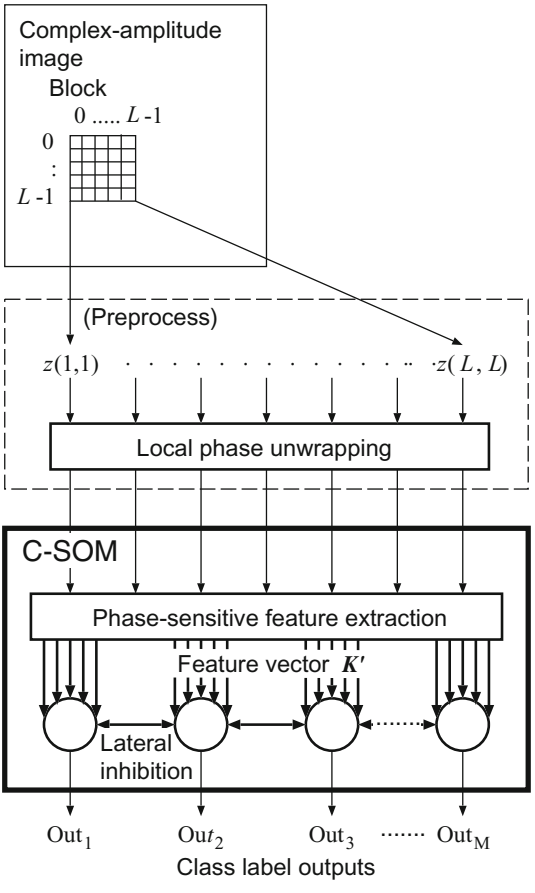

Fig. 5.5 Construction of the adaptive interferometric-radar-image segmentation system based on complex-valued self-organizing-map (CSOM). Reprinted from Fig.2 in [197] in the caption of Fig.5.2 with permission from IEICE.

not so important, or should rather be suppressed in the classification process to make a mountain area "mountain." For this reason, we slightly modify $\boldsymbol{K}$ into $\boldsymbol{K}'$ in such a way that the covariance is insensitive to the positive and negative of the phase differences as

$$\boldsymbol{K}' \equiv [M, K(0,0), K'(0,1), K'(1,0), K'(1,1)] \tag{5.6}$$

$$K'(\xi,\eta) = |K(\xi,\eta)| \ e^{j|\varphi(\xi,\eta)|} \tag{5.7}$$

where we write $K \equiv |K(\xi,\eta)| \ e^{j\varphi(\xi,\eta)}$. We adopt such fine customization in the feature vector according to the purposes.

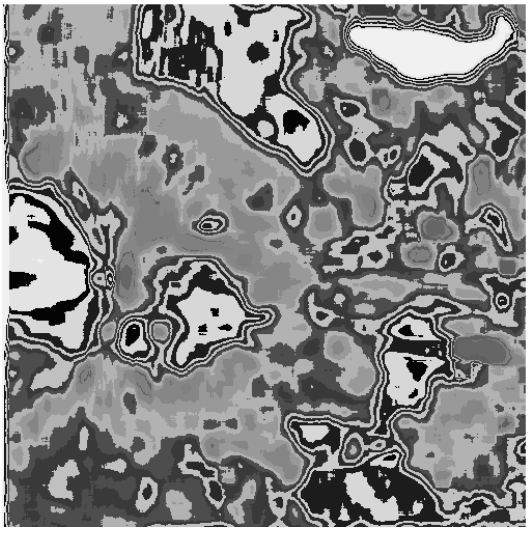

(a)

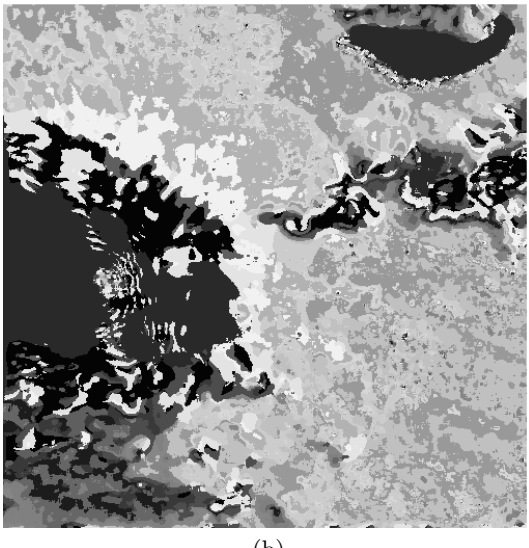

(b)

Fig. 5.6 Adaptive segmentation results for the InSAR land image generated by (a)a conventional SOM system and (b)the proposed CSOM system. Reprinted from Figs.5 and 6 in [197] in the caption of Fig.5.2 with permission from IEICE.

5.5 Generation of Land-Surface Classification Map

Figure 5.2 is a radar-image example obtained at an area around Mount Fuji and Lake Yamanaka, Japan. Figure 5.2(a) shows amplitude, while Fig.5.2(b)

shows phase, both in gray scale. We find that the reflection is very small at Lake Yamanaka and relatively small at forests and rocky areas. On the other hand, in the phase map, though the contours are apparently similar to the contours that should be found in an elevation map, the phase at the Lake is unnaturally turbulent because the low reflectance relatively emphasizes measurement noise.

Figure 5.6 shows the segmentation results (a)generated by a conventional (real-valued) SOM system for the amplitude image, and (b)generated by the proposed CSOM system for the complex-amplitude image. In 5.6(a), we find that Lake Yamanaka, forests, and rocky areas are segmented from others. On the other hand, in Fig.5.6(b), we find that the mass of Mount Fuji and the mountain ridge near Lake Yamanaka are also segmented additionally to those above, showing the fine folds of the skirt of Mount Fuji. In this way, we can generate a more useful adaptively segmented map by incorporating phase information into the segmentation with the concept of the phase-sensitive superbrain.

5.6 Summary

In this chapter, we described the usefulness of the complex-valued neural network to segment adaptively the land surface. This method is now going to be applied to wide areas such as inspections in factories. Complex-amplitude signals are of wide use in high-resolution ranging systems. They are also important in imaging permittivity distribution, e.g., with phase-contrast microscope. In such applications, the above-mentioned ideas are quite useful to realize adaptive processing.